Machine Learning for search for new resonances with ATLAS at the LHC - Project Plan

Dennis Lindebaum

December 10, 2020

1 Introduction

The question of dark matter, which accounts for about 85% of the matter in the universe [1], has gone unanswered for decades. One set of theories predict new massive Z' bosons which can couple both to visible matter and dark matter, such as those put forth in [2–5]. A peak in the number of scattering events would appear around the boson's mass. If the mass of the boson is small, then the peak will occur at a low energy, but this low energy regime already has many scattering events caused by QED and QCD interactions. Both of these interactions have massless propagators, leading to a very large cross section at low energies. If there is a signal present from a Z' bosons, it is necessary find observables to separate signal from background.

Searches for such low mass bosons have already been carried out by the ATLAS Collaboration [6] and CMS Collaboration [7]. Both of these searches were carried out on $\sqrt{s} = 13$ TeV data from 2015-2017. Neither of these searches were able to find evidence for any new bosons coupling to quarks, however the LHC continued to run for months after these analyses were carried out. It is worth re-testing these hypotheses with the new data to confirm nothing new has appeared in subsequent data.

The aim of this project is to find new observables which can be used to better discriminate the events we are searching for from background events. In this report, the relevant details regarding the method of the search are presented to show how these new observables can assist the search. It will also outline the method of obtaining these observables and give an expected time frame over which the project will be carried out.

2 Search strategy

2.1 ISR + boosted events

To probe for bosons with small masses (of order 10^2 GeV), it is necessary to search for specific events in which much of the initial energy has been carried away by Initial State Radiation (ISR). The centre of mass energy $\sqrt{s} = 13$ TeV at the LHC can create very high energy events. Low energy collision produce lower momenta products which are discarded to keep the event rate low enough for recording software. The ISR ensures enough energy is present to pass the detector triggers which are in place to prevent signal overload from low energy QCD scattering with a high cross section. The "boosted" criteria requires the ISR, and subsequently the decay products, to be boosted in the transverse direction, perpendicular to the beam lines. These criteria allow for probing of low energy events with high beam energies and have characteristics to allow them to be separated from other background events which may appear similar, but do not fit the ISR + boosted criteria.

A 'perfect' ISR + boosted event is shown in figure 1. Two characteristic jets are seen. A narrow jet, coming from the ISR, and a large-R jet, coming from the decay event. The jets are determined by the anti-k_t algorithm [8], explained further in section 3.1.2. The Feynman diagram for such an event is shown in figure 2. The initial state has only a quark anti-quark pair, the anti-quark must come from the sea quarks of one of the protons. Additional jets will

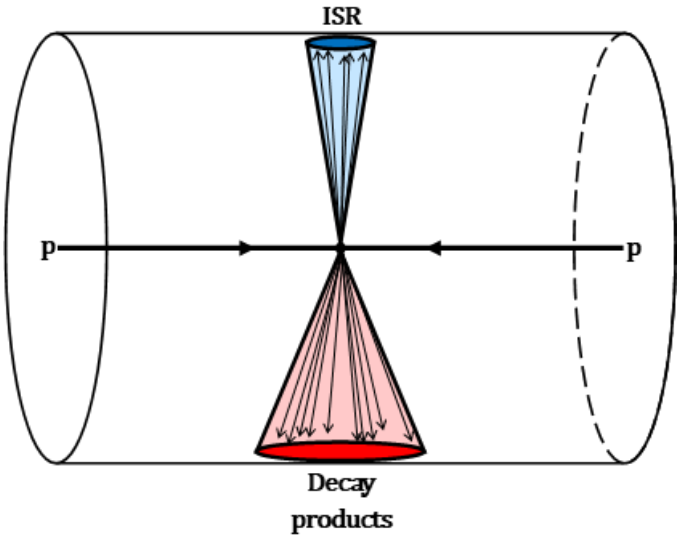

Figure 1: Cartoon plot of an idealised ISR + boosted event. The protons from the incoming beams collide at the centre of the detector and create two jets. The smaller radius jet (red) corresponds to initial state radiation and the larger radius jet (blue) corresponds to the products of the decay of a massive boson created in the collision. The jets are both boosted in the transverse direction.

be caused by the other quarks in the incident protons and pile-up from other events in the same bunch crossing. The example in figure 1 would include many additional jets, but the highlighted jets will have much larger transverse momenta and are used to identify and measure the event.

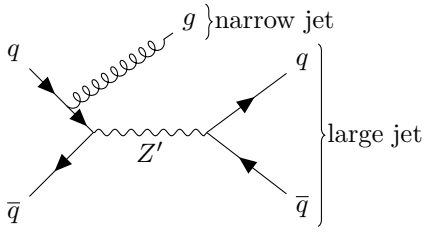

Figure 2: Feynman diagram showing the leading order ISR event considered. One of the incident quarks undergoes initial state radiation boosted in the transverse direction, releasing a gluon, seen as a small radius jet. The collision produces the dark matter mediator Z', also boosted in the transverse direction. This boson decays to a quark anti-quark pair which is detected as a large radius jet.

2.2 Background events

Two types of background events will be present. Resonant events which include ISR, but contain only standard model physics and events which do not include ISR, but share similarities in signal with the characteristics of ISR when sufficiently boosted.

ISR background events are given by replacing the hypothetical Z' boson with a standard model propagator. The strongest coupling we have for this process is from QCD with a gluon as a propagator. Electroweak processes will also contribute, but the weaker coupling means that these processes will be less significant. An exception to this is around the mass of the Z and W bosons, where resonance increases the interaction cross section. The ISR processes can also vary by the boson causing the ISR, which could be a W, Z or γ, however this is also true of Z'

mediated events. Since the QCD coupling is larger than electroweak coupling, we will continue to show the ISR as radiation of a gluon. A collection of the lowest order ISR which contribute to the background is given in figure 3.

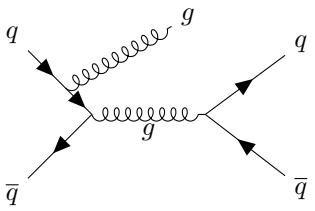

(a) Gluon mediated

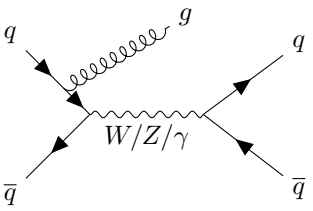

(b) Electroweak mediated

Figure 3: Feynman diagrams showing the leading order ISR events which contribute to background in the search for a new Z' boson.

Additional processes which may look like ISR events are dijet events. Dijet processes begin at a lower order than the ISR processes, so are more likely to occur. Removing as many of the dijet processes as possible increases the signal to background ratio, reducing the uncertainty, and is the goal of this project.

Figure 4 shows some examples of leading order dijet events which can be boosted in the transverse direction. Of these scattering processes, t-channel events are less likely to be boosted because the propagator requires higher momentum and is further off-shell. Figure 4d highlights the top quark decay process. This is included because the dominant decay of a top quark can lead to similar jets to an ISR event. The heavy bottom quark can result in a large radius jets similar to that expected from a Z' boson.

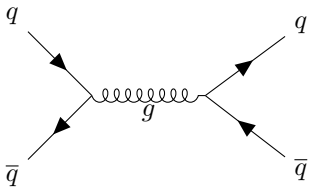

(a) Gluon s-channel

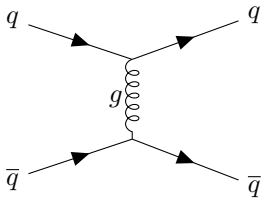

(b) Gluon t-channel

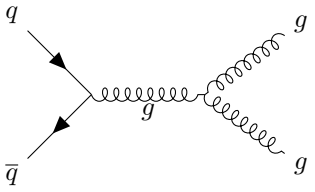

(c) Gluon - gluon production

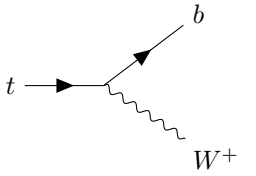

(d) Top quark decay

Figure 4: (a) to (c): Feynman diagrams showing some of the leading order dijet processes which contribute to background in the search for a new Z' boson. (d): The most likely decay channel of a top quark. This has a similar signal to an ISR event.

The expected results of all known background processes must be simulated so it can be compared to experimental data. Deviations of the experimental data from the predicted background can indicate new physics, such as the hypothetical Z' boson.

Monte-Carlo simulation techniques, such as those used in Sherpa [9], produce very accurate predictions of standard model physics. The outputs of these simulations give a probability distribution for different events, including parameters such as jet energies and angles. The same tagging processes are applied to both the experimental and simulated data-sets to ensure the simulated and experimental backgrounds match.

3 Method

3.1 Detection basics

3.1.1 ATLAS detector

The data considered is taken from the ATLAS collaboration. Measurements are made in a cylindrical detector positioned around the interaction point, described in detail in [10]. Figure 5 shows an overview of the detector. The signature of the ISR + boosted events chosen are entirely hadronic, and a brief discussion of the relevant components is included. These are the hadronic calorimeters and the trackers and associated magnetic fields.

The ATLAS detector contains a solenoidal magnet on the interior and sets of toroidal magnets at a larger radius from the beam. Hadrons will not reach a large enough radius to be significantly affected by the toroidal magnets. The smaller solenoid creates a magnetic field parallel to the beam line. This means charged particles will curve in a plane perpendicular to the beam line dependent on their momentum and charge.

The inner detector, found inside the solenoid is a tracking system. This is a series of layers of detectors which can detect a charged particle moving through it with little effect on the momentum of the particle detected. This allows for reconstruction of particle tracks as they travel through the inner detector. For hadron jets, this is important in determining the origin of the jet, which may be at a distance from the collision point if produced by the decay of a propagator of finite lifetime, but such analysis is beyond the goals of this project.

Calorimeters are located outside the inner detector and solenoid. They are designed to completely stop the particles and measure the energy deposited as the particle stops. There are two types of calorimeter. Electromagnetic calorimeters (ECAL) which specialise in stopping electrons and photons and hadronic calorimeters (HCAL) which specialise in stopping hadrons. Hadrons passing the ECAL will deposit a small fraction of their energy, but are not entirely stopped. For this reason, the HCAL is placed further from the beam centre than the ECAL. When reconstructing the 4-momentum contributed by an ECAL or HCAL cell, it is assumed the measured particles are in the relativistic limit so their energy is equal to their momentum, $E \approx |\vec{p}|$.

The output of the HCAL is most easily viewed as a set of momenta measured as a function

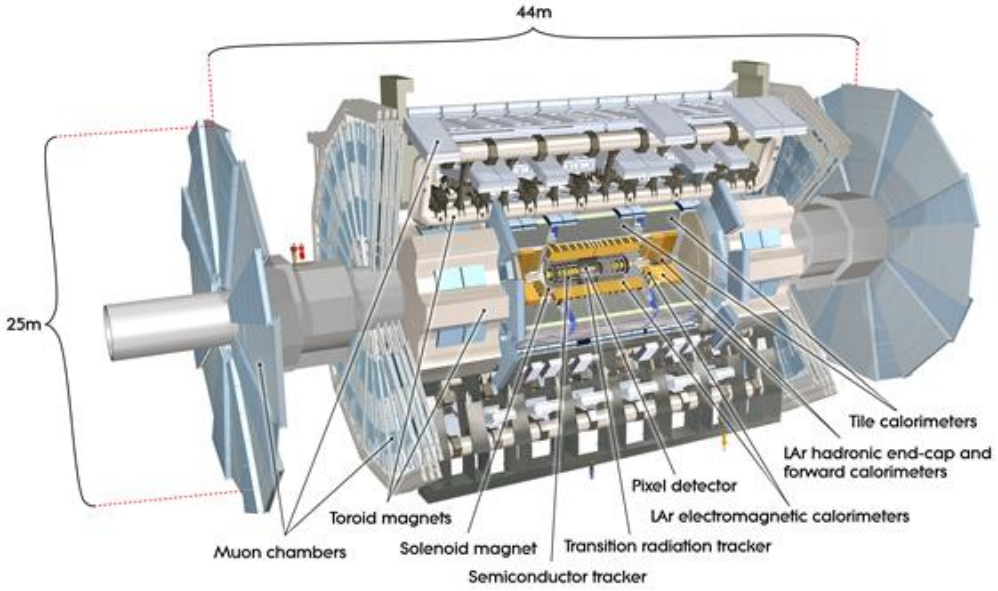

Figure 5: Diagram of the components of the ATLAS detector. Taken from [11].

of position on the 2D surface around the beam to indicate the direction. This surface is conventionally described using pseudorapidity, η, and azimuth, ϕ. The azimuth is taken as the angle covering 0 to 2π around the axis of the beam. Pseudorapidity is defined as $\eta \equiv -\ln[\tan(\theta/2)]$. This describes all the relevant hadronic measurements for this project.

3.1.2 Measured variables

The data from the detector must receive further processing before it can be used. Jet clustering algorithms group together energy deposits in the calorimeter as jets which can be linked to a particle or propagator. Adding together all the 4-momenta in a jet gives a value for the 4-momentum of the jet's source.

Various methods exist for clustering jets. The algorithm predominantly used in this project is the anti-k_t algorithm [8], for which an example clustering is shown in figure 6.

The jet clustering algorithms are run around energy deposits satisfying a minimum energy excess over the background low energy noise. Nearby energy deposits will then be included in the jet if they have sufficient energy above the background and satisfy the jet criteria of belonging to the jet. There is a free radius parameter, R, in the clustering algorithms which affects the size of the jets An event can be clustered at different radii to give multiple sets of jets with each set containing the same total energy. Selection requirements can be applied to jets of a certain radius only. In this project, the requirements eventually lead to a unique choice of which jets to use as large-R jets and which to use as narrow jets.

After jet clustering algorithms have been carried out, the result is multiple sets of jets of different radii. Each jet will have a measured 4-momentum. This contains the direction, energy, momentum and invariant mass of the jet.

3.2 Tagging ISR + boosted events

The clustered data will have cuts applied which exclude data which clearly do not match the requirements of ISR + boosted events. Before cuts are made, the large-R jets are trimmed [12]. In this process, clustering with a much smaller radius parameter is carried out within the large-R jet. These smaller jets are discarded if they do not carry a sufficiently large fraction of the initial transverse momentum of the jet. This is done to reduce the effects of pile-up coming from simultaneous low energy events.

The ISR requirement needs a narrow jet of high energy to be present. Running the anti-k_t algorithm with a radius of $R = 0.4$ (narrow jet), we require at least one jet with this radius

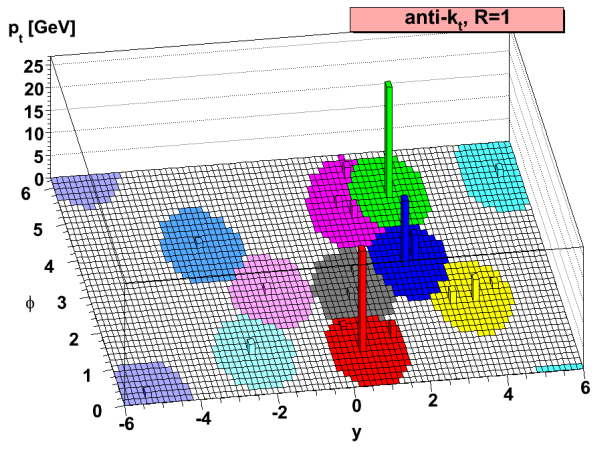

Figure 6: Example of clustering of jets within a sample event using the anti-k_t algorithm. Taken from [8].

.

parameter to have a minimum transverse momentum, $p_T > 380$ GeV [6].

Topological requirements can then be applied to the data. The cylindrical ATLAS detector has better accuracy along the barrel of the detector. Different requirements are applied to the large-R and narrow jets. Large-R jets are required to have $|\eta| < 2.0$ and narrow jets to have $|\eta| < 2.4$ to ensure good detection. This is consistent with boosted events which must have a high transverse momentum. Additionally, if these jets come from the same event, we should expect them to appear on opposite sides of the beam and have similar momenta due to conservation of momentum. The previous ATLAS search required to have a large-R jet to be present which has an azimuthal angular separation of $|\Delta\phi| > \pi/2$ from a candidate narrow radius jet satisfying the momentum requirements. It is also required that the large-R jet satisfy $p_T > 450$ GeV to ensure the transverse momentum is close to that of the narrow jet.

τ_{21}^{DDT}, is introduced [13]. This is a constructed observable which has been decorrelated from the mass of the jet that probes the substructure of the jet. It should have a smaller value in the jet which is closer in appearance to two subjets making up a larger jet. It is expected to see this substructure in the large-R jet, so this can be used to determine which jet is large-R if multiple candidate jets are present and to discard events if τ_{21}^{DDT} is too large.

4 Project goal

The selection criteria for events described in section 3.2 go some way to excluding events without ISR, but the selection can be improved by using additional decorrelated variables, such as τ_{21}^{DDT} explained in section 3.2. Additional decorrelated observables have been constructed involving energy correlations and functions thereof [14–16]. A good observable in the context of the project will have a distinct separation between jets originating from the decay of a boson and single jets from other background events which do not contain ISR.

Decorrelation is important to ensure the separating power of the observable does not change as the mass of the large-R jet changes, which is the discriminant used in plotting event frequencies. Machine learning techniques will be used to construct new variables from current observables whilst ensuring the result is decorrelated.

Achieving this goal will first require familiarity with the current decorrelated variables used and how their effectiveness if determined. Creating the Adversarial Neural Networks to find these variables is the core of the project and will produce the new candidate observables. These observables must then be tested to determine their effectiveness compared to the currently used

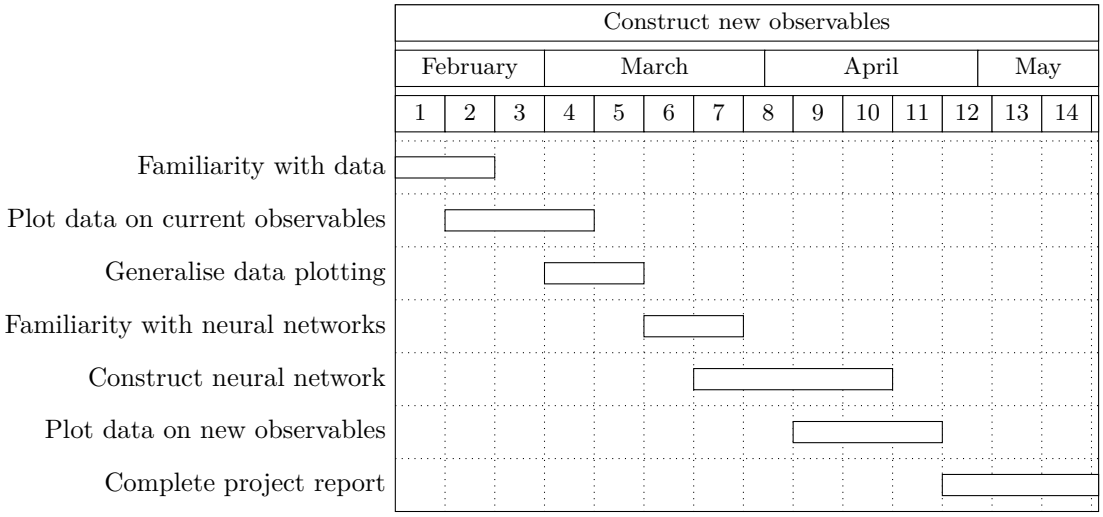

Figure 7: Gantt chart showing a breakdown of steps and estimated time frame in weeks to construct new observables for low mass boson detection. The chart assumes the background reading has already been completed and begins near the start of Lent term.

variables. Figure 7 shows a summary of these steps and the expected time frame in which the project will be completed. The Gantt chart starts in Lent term assuming that the prerequisite background reading has been completed.

References

[1] Gianfranco Bertone, Dan Hooper, and Joseph Silk. "Particle Dark Matter: Evidence, Candidates and Constraints". In: *Phys.Rept.405:279-390,2005* (Apr. 21, 2004). DOI: 10.1016/j.physrep.2004.08.031. arXiv: hep-ph/0404175 [hep-ph].

[2] David London and Jonathan L. Rosner. "Extra gauge bosons in E_6". In: *Phys. Rev. D* 34 (5 Sept. 1986), pp. 1530–1546. DOI: 10.1103/PhysRevD.34.1530. URL: https://link.aps.org/doi/10.1103/PhysRevD.34.1530.

[3] Paul Langacker. "The Physics of Heavy Z' Gauge Bosons". In: *Rev.Mod.Phys.81:1199-1228,2009* (Jan. 9, 2008). DOI: 10.1103/RevModPhys.81.1199. arXiv: 0801.1345 [hep-ph].

[4] Ennio Salvioni, Giovanni Villadoro, and Fabio Zwirner. "Minimal Z' models: present bounds and early LHC reach". In: *JHEP 0911:068,2009* (Sept. 7, 2009). DOI: 10.1088/1126-6708/2009/11/068. arXiv: 0909.1320 [hep-ph].

[5] Haipeng An, Ran Huo, and Lian-Tao Wang. "Searching for Low Mass Dark Portal at the LHC". In: *Phys.Dark Univ. 2 (2013) 50-57* (Dec. 10, 2012). DOI: 10.1016/j.dark.2013.03.002. arXiv: 1212.2221 [hep-ph].

[6] ATLAS Collaboration. "Search for light resonances decaying to boosted quark pairs and produced in association with a photon or a jet in proton-proton collisions at $\sqrt{s} = 13$ TeV with the ATLAS detector". In: *Phys. Lett. B 788 (2019) 316* (Jan. 26, 2018). DOI: 10.1016/j.physletb.2018.09.062. arXiv: 1801.08769 [hep-ex].

[7] CMS Collaboration. "Search for low mass vector resonances decaying into quark-antiquark pairs in proton-proton collisions at $\sqrt{s} = 13$ TeV". In: *Phys. Rev. D 100, 112007 (2019)* (Sept. 9, 2019). DOI: 10.1103/PhysRevD.100.112007. arXiv: 1909.04114 [hep-ex].

[8] Matteo Cacciari, Gavin P. Salam, and Gregory Soyez. "The anti-k_t jet clustering algorithm". In: *JHEP 0804:063,2008* (Feb. 8, 2008). DOI: 10.1088/1126-6708/2008/04/063. arXiv: 0802.1189 [hep-ph].

[9] T. Gleisberg et al. "Event generation with SHERPA 1.1". In: *JHEP 0902:007,2009* (Nov. 27, 2008). DOI: 10.1088/1126-6708/2009/02/007. arXiv: 0811.4622 [hep-ph].

[10] ATLAS Collaboration. "The ATLAS Experiment at the CERN Large Hadron Collider". In: *Journal of Instrumentation* 3.08 (Aug. 2008), S08003–S08003. DOI: 10.1088/1748-0221/3/08/s08003.

[11] Joao Pequenao. "Computer generated image of the whole ATLAS detector". Mar. 2008. URL: https://cds.cern.ch/record/1095924.

[12] David Krohn, Jesse Thaler, and Lian-Tao Wang. "Jet Trimming". In: *JHEP 1002:084,2010* (Dec. 8, 2009). DOI: 10.1007/JHEP02(2010)084. arXiv: 0912.1342 [hep-ph].

[13] James Dolen et al. "Thinking outside the ROCs: Designing Decorrelated Taggers (DDT) for jet substructure". In: *JHEP 05 (2016) 156* (Feb. 29, 2016). DOI: 10.1007/JHEP05(2016)156. arXiv: 1603.00027 [hep-ph].

[14] Andrew J. Larkoski, Gavin P. Salam, and Jesse Thaler. "Energy Correlation Functions for Jet Substructure". In: (Apr. 30, 2013). DOI: 10.1007/JHEP06(2013)108. arXiv: 1305.0007 [hep-ph].

[15] Ian Moult, Lina Necib, and Jesse Thaler. "New Angles on Energy Correlation Functions". In: (Sept. 23, 2016). DOI: 10.1007/JHEP12(2016)153. arXiv: 1609.07483 [hep-ph].

[16] Andrew J. Larkoski, Ian Moult, and Duff Neill. "Power Counting to Better Jet Observables". In: (Sept. 22, 2014). DOI: 10.1007/JHEP12(2014)009. arXiv: 1409.6298 [hep-ph].